



Operating Conditions of a Single-Chamber SOFC

Teko W. Napporn,^{a,*} Xavier Jacques-Bédard,^a François Morin,^b and Michel Meunier^a

^aDépartement de Génie Physique, École Polytechnique de Montréal, Québec H3C 3A7, Canada

^bInstitut de Recherche d'Hydro-Québec, Varennes, Québec J3X 1S1, Canada

Single-chamber cells of two different types have been operated between 700 and 800°C in various methane-air mixtures. These cells are made mostly of conventional materials for solid oxide fuel cells (SOFCs), strontium-doped lanthanum manganite, yttria-stabilized zirconia (YSZ), and Ni-YSZ cermet. One type is electrolyte-supported, while the other represents a state-of-the-art fabrication for anode-supported cells. The anode-supported cells operate in a narrower range of methane-air ratios, but offer remarkable maximum specific powers, 360 and 285 mW/cm² at 800 and 700°C, respectively. Some theoretical considerations about the actual operation of these cells are also provided.

© 2004 The Electrochemical Society. [DOI: 10.1149/1.1814034] All rights reserved.

Manuscript submitted February 10, 2004; revised manuscript received May 11, 2004. Available electronically November 1, 2004.

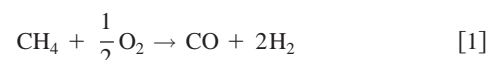
The idea of a single chamber fuel cell was suggested several decades ago by Eyraud *et al.*¹ based on some initial experimental evidence at room temperature. This promising concept was further investigated by van Gool.² But it was only quite recently that a single-chamber fuel cell based on solid oxide materials and a methane-air mixture was developed to deliver a significant current.³ This first cell operated at 950°C with a 8YSZ electrolyte (8 % mol Y₂O₃-ZrO₂), a gold cathode, and a nickel cermet anode; it delivered a maximum power of 2.4 mW/cm². Hibino and coworkers⁴ also demonstrated the feasibility of an alternate design with both electrodes on the same side of the solid electrolyte, a design already suggested within the literature.^{2,5} Since then, most cell improvements have resulted either from a surface modification of the electrolyte or from further modifications of both electrode compositions. Asano and Iwahara obtained a maximum specific power of 50 mW/cm² by pretreating their YSZ electrolyte to form an initial Pr₆O₁₁ layer.⁶ By adding MnO₂ to their La_{0.8}Sr_{0.2}MnO₃ (LSM20) cathode, substituting 8YSZ by Ce_{0.8}Gd_{0.2}O_{1.9} (GDC20) within their cermet anode, and still maintaining a methane-to-oxygen ratio, R_{mix} , equal to two, Hibino and coworkers⁷ increased their cell performance to 162 mW/cm² at 950°C. Their most remarkable cell performance, however, was recently obtained at 550°C⁸ with a maximum specific power equal to 644 mW/cm². Such a performance was attributed to various contributive factors: (i) the addition of PdO to the anode, (ii) the change of previous cell materials to Sm_{0.5}Sr_{0.5}CoO₃ (SSC50), Sm_{0.2}Ce_{0.8}O_{1.9} (SDC20) and Ni-30%SDC20 for the cathode, the electrolyte and the anode, respectively, (iii) a change of R_{mix} down to one and, finally, (iv) the use of a much thinner electrolyte. The latter cell performance makes the single-chamber solid oxide fuel cell a promising avenue for new cell designs that should lead to practical applications.

Meanwhile, a first attempt⁹ to reproduce the initial results from Hibino and coworkers³ failed in reporting better performances. However, cell performances approaching those of Hibino and coworkers⁷ were recently reported, taking into account the use of rather conventional cell materials and a lower nominal operating temperature.¹⁰ On the other hand, the concept of the single-chamber fuel cell has attracted new theoretical work in relation with solid oxide fuel cells (SOFCs).¹¹⁻¹³ Despite the attractiveness of such a concept, several questions remain to be addressed to make it fully practical. One of these is the actual behavior of an unstable gas-mixture upon the electrodes and the actual mechanisms implied therein. The efficiency that could eventually be reached is another important consideration with this type of cell. Moreover, some ex-

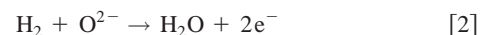
perimental details from previous studies still need further clarification. The present study pays close attention to the experimental conditions and to some of the questions raised above.

Theory

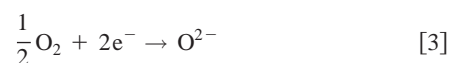
Thermodynamically speaking, the methane/air mixture is essentially unstable. It would normally be rapidly brought up to the cell at high temperature in Fig. 1 before any significant reaction occurs. When the methane-to-oxygen ratio, R_{mix} , equals 2, as for most early experiments on the single chamber SOFC,^{3,6,15} the sole reaction that also avoids carbon deposition is



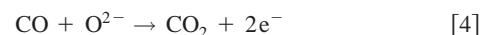
This partial oxidation reaction is important on a general basis for the production of synthetic gas. In regard to the single-chamber fuel cell, Reaction 1 is expected to occur heterogeneously upon the cermet surface. It should then act as a hydrogen provider for the anode interface with the electrolyte. The electrochemical reaction at this interface then is



Meanwhile, the cathode is mostly sensitive to the oxygen component. The oxygen would react directly with the cathode as



Incidentally, drawing an electrical current at an initial value of $R_{\text{mix}} = 2$ makes the mixture globally richer in methane because of the additional oxygen consumption due to Reaction 3. As R_{mix} becomes smaller than 2, *i.e.*, for mixtures initially richer in oxygen, the formation of carbon dioxide is expected. One additional electrochemical reaction may then need to be considered at the anode



However, according to Appleby,¹⁴ this electrochemical reaction obeys a much slower kinetics than Reaction 2, the former reaction with hydrogen being basically prevalent in high-temperature fuel cells. With mixtures at $R_{\text{mix}} < 2$, the question also arises about the proportions between the various reaction products, water vapor, carbon monoxide and carbon dioxide adding to the initial reactants and hydrogen. Several chemical reactions may be written that interrelate the formation of these products, but no full chemical equilibrium is expected while the single-chamber cell needs the mixture to stay out of equilibrium for a voltage to be produced. Nonetheless, starting from the voltage generated under open-circuit conditions, E_0 , it is

* Electrochemical Society Active Member.

^z E-mail: teko.napporn@polymtl.ca

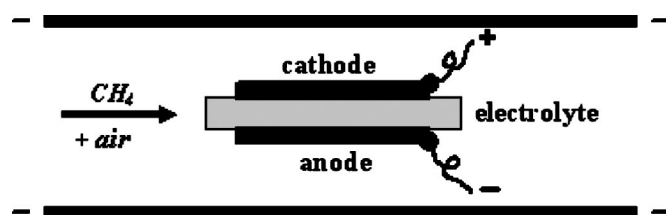


Figure 1. Simplified schematic of a single-chamber solid oxide fuel cell.

still possible to describe the oxygen partial pressure existing at each electrode interface with the electrolyte. The usual equation for an oxygen concentration cell thus reads

$$E_0 = (RT/4F)\ln[(p_{O_2})_c/(p_{O_2})_a] \quad [5]$$

where F , R , and T stand for the Faraday constant, the molar gas constant, and the absolute temperature, respectively, and $(p_{O_2})_c$ and $(p_{O_2})_a$ are the oxygen partial pressures prevailing at the cathode and the anode, respectively. At the cathode, the oxygen partial pressure is equal or somewhat smaller than the initial oxygen concentration within the reactive mixture. In a methane-air mixture, this leads to values of $(p_{O_2})_c \leq 0.17$ – 0.13 atm for R_{mix} between 1 and 2.

Cell efficiency.—The cell efficiency is normally understood as the useful power generated by a specific cell with respect to the fuel input, specifying low or high heat values for the fuel. Such a definition is more specifically useful for a fully integrated system and may include some type of cogeneration. For the rather nonconventional single-chamber fuel cell, a more limited approach has recently been put forward,⁸ considering Eq. 4 as the prevailing reaction at the anode at $R_{\text{mix}} = 1$ and then dividing the maximum specific power drawn from the cell, P_{max} , by the total heat rate due to such a reaction. Approximately the same result would have been obtained without making that assumption about Eq. 4 just by considering the various reaction enthalpies at $R_{\text{mix}} = 1$. Whether water vapor, carbon monoxide, or carbon dioxide, or any combination of these, are favored, full oxygen consumption at $R_{\text{mix}} = 1$ does not lead to a large variation of the overall heat of reaction, ΔH_{react} . For example, at 800°C, ΔH_{react} ranges from -270 to -305 Kjoules/mole of CH_4 depending upon the proportions between the various reaction products.¹⁶ Thus, for a preliminary evaluation of the single-chamber fuel cell, one may use the following relationship for the fuel utilization (F.U.) factor

$$F.U. = P_{\text{max}}/\Delta H_{\text{react}} \quad [6]$$

where ΔH_{react} represents the enthalpy of reaction for the overall reaction corresponding to full oxygen consumption from the mixture at the undergoing R_{mix} value, and P_{max} is the corresponding power drawn from the cell with the gas mixture passing only once through the cell compartment. It is clear for the single-chamber cell that the best fuel utilization can only occur at the maximum specific power. Also, any unburned oxygen contributes in lowering the fuel utilization factor. Finally, a higher R_{mix} value up to 2 may favor a higher fuel utilization factor due to a correspondingly lower ΔH_{react} . But this would be valuable only if the remaining unburned fuel is usefully recycled.

Experimental

Fabrication.—Conventional SOFC materials related to those in Ref. 7 are used for the main cell components. The $\text{La}_{0.8}\text{Sr}_{0.2}\text{MnO}_3$ powders for the cathode have been supplied by Praxair and, alternatively, by NexTech. The 0.20 mm thick 8YSZ electrolyte has been provided by Performance Ceramics. The cermet slurry consisting of a Tosoh TZ-8Y powder, ball-milled with a fine NiO powder from Baker (nickelous oxide no. 2796-01), is prepared according to a

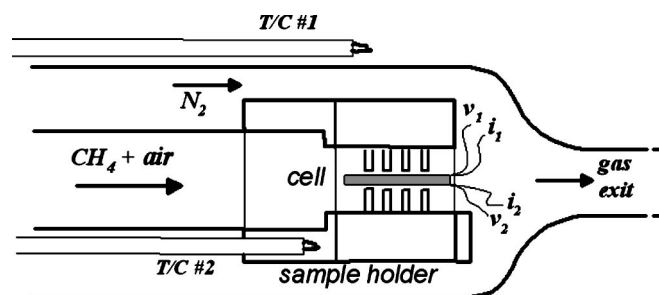


Figure 2. High-temperature set-up and gas flow path around the single-chamber cell.

state-of-the-art procedure,¹⁷ the composition in terms of weight ratios being basically 55% nickel oxide/45% YSZ. Slurries of both electrodes are tape casted onto the electrolyte to form thin coatings. Firing at 1250°C for 3 h results in electrode layers approximately 10–20 μm thick with electrode areas of approximately 8×8 mm in size. $\text{La}_{0.8}\text{Sr}_{0.2}\text{Fe}_{0.2}\text{Mn}_{0.8}\text{O}_3$ (LSFM22) and $\text{La}_{0.5}\text{Sr}_{0.5}\text{MnO}_3$ (LSM50) have been alternatively used for the cathode. In addition, thicker anode-supported cells have been commercially provided by InDEC B.V.. These latter cells represent a state-of-the-art fabrication for using in conventional SOFCs. They are nominally made of Ni-YSZ/8YSZ/(La, Sr)MnO₃ with layer thicknesses not greater than 600, 10, and 60 μm , respectively. Ni-YSZ is very close to the cermet composition above and (La, Sr)MnO₃ has a composition very close to LSM20. Coupons of the right size were cut out and tested in our experimental set-up in the same manner as the above electrolyte-supported cells.

Set-up.—Special attention was paid to the gas flow around the cells and to the actual current collection. Details of our experimental set-up are described in Fig. 2 which departs from the basic description found elsewhere.^{3,7,8} A sample holder machined out of a Macor block is used to specifically constrain the methane/air mixture directly around the sample; nitrogen acting as a blanket additionally flows at about 700 sccm (cm^3/min STP). This ensures that no counterdiffusion occurs and that the incoming reactive mixture is rapidly flushed away passed the sample holder. The outer and inner quartz tubes have inner diameters equal to 37 and 10.5 mm, respectively. The cell is pressed between two gold meshes and the gas mixture allowed to flow on both sides. Bare platinum meshes and wires are totally avoided due to the platinum high catalytic activity in regard to methane. Instead, gold wires and meshes are used within the cell chamber. To let the gas flow freely and uniformly around the cells, teeth are equally machined out on both parts of the sample holder. These teeth are also regularly spaced in a quincunx fashion. To fully ensure a good electrical contact, a thick impervious gold pattern is screen printed on each electrode starting from a laser-cut stencil with slots 0.10 mm wide and a gold paste Heraeus C5450. Taking this pattern into account leads to an effective electrode area of about 0.50 cm^2 . The cermet is initially reduced at 800°C and $R_{\text{mix}} = 2$ immediately before operating the cells at various temperatures and R_{mix} values. The inner gas mixture normally flows at 350 sccm STP. Polarization curves are established stepwise with an active current sink and the voltage is monitored through the reference wires exiting from the cell.

Temperature monitoring.—Due to the ongoing chemical reactions, the actual cell temperature may be at variance with its nominal operating temperature. The furnace temperature is controlled through a thermocouple (TC 1) outside the outer silica tube and it is also monitored with a second thermocouple (TC 2) placed into the Macor sample holder (Fig. 2). To more closely evaluate purely catalytic effects within the single-chamber cell, overheating was fol-

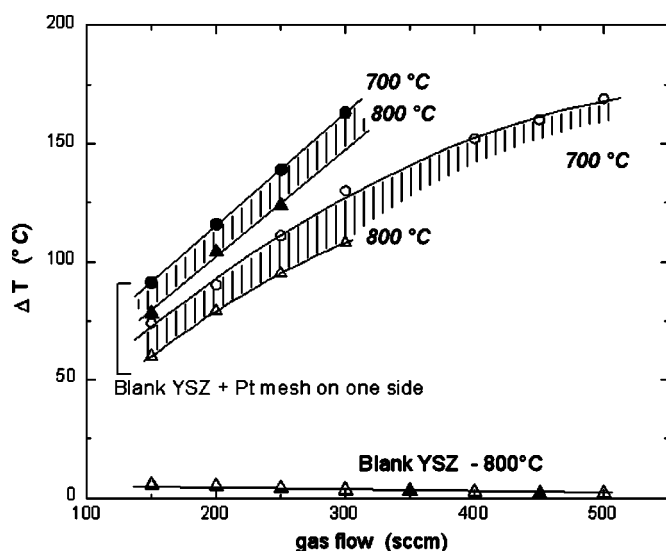


Figure 3. Overheating of blank YSZ platelets at various furnace temperatures either with or without an added platinum mesh. Filled symbols stand for $R_{\text{mix}} = 1$ and empty symbols for $R_{\text{mix}} = 2$.

lowed independently for various cell components under flowing methane/air mixtures. Various samples were prepared starting from $11 \times 11 \times 0.2$ mm YSZ platelets as follows.

A fine gauge thermocouple, .003 in. in diameter type R, was totally embedded on one side of the platelets by means of a light coating of YSZ-based cement. The wires further exited through a thin alumina capillary also coated with the YSZ-base cement to protect the thermocouple from any direct contact with the flowing methane/air mixture. The other side of the YSZ platelets was either left blanked, covered with a 8×8 mm gold or platinum (Aesar no. 10283 or equiv.) mesh, or, finally, with a cathodic or an anodic coating of equivalent size. After placing the sample within the sample holder, the actual platelet temperature was directly followed in various flowing methane-air mixtures and in nitrogen.

Results

Overtemperatures.—Platinum exerts a strong effect upon the true cell temperature as suspected above and as shown in Fig. 3. ΔT represents the difference between the actual sample temperature and the furnace temperature. ΔT is larger at the lower R_{mix} value equal to one in accordance with a potentially greater oxygen consumption. A more or less linear increase of temperature also occurs with increasing gas flow. With platinum, the upper limit upon the gas flow is dictated here by the need not to exceed a certain sample temperature to maintain full integrity of our samples and complete reversibility of the results. Overtemperatures are slightly more important at 700°C. This is probably due to less effective radiative heat losses of the sample with the environment, including the sample holder, at this lower furnace temperature. The temperature rise at any temperature is almost instantaneous and it looks very much like an ignition process. As opposed to platinum, blank samples overheat negligibly at all gas flows up to and including 800°C. This again holds when a gold mesh is applied to a blank sample, justifying then the exclusive use of gold as a current collector within the present study. A certain amount of overheating is found for cermet anodes in Fig. 4a although much smaller than for platinum. The tendency for increasing overtemperatures with increasing gas flow is maintained. In contrast to platinum, $R_{\text{mix}} = 2$ leads to a somewhat greater effect than $R_{\text{mix}} = 1$. It may be indicative of distinct oxidative reactions going on upon the cermet surface as compared to platinum. Overheating due to cathodes in Fig. 4b is smaller than for cermets although not totally negligible.

Electrolyte-supported cells.—The performance of a typical cell with a LSM20 cathode is illustrated in Fig. 5. Immediately following the initial cermet reduction, this cell exhibits an open circuit voltage (OCV) exceeding 1.02 V, a short-circuit current close to 400 mA/cm² and a maximum specific power equal to 85 mW/cm². The OCV varies only slightly in the next polarization curves at lower temperature. But the short-circuit current diminishes significantly although a short-circuit current close to 200 mA/cm² can still be drawn at 700°C. The last curve, back at 800°C, comes out from the same cell after 3 h of operation and an intermediate cool down in pure nitrogen to room temperature. There has been an obvious performance loss during the operation of these cells. All our electrolyte-

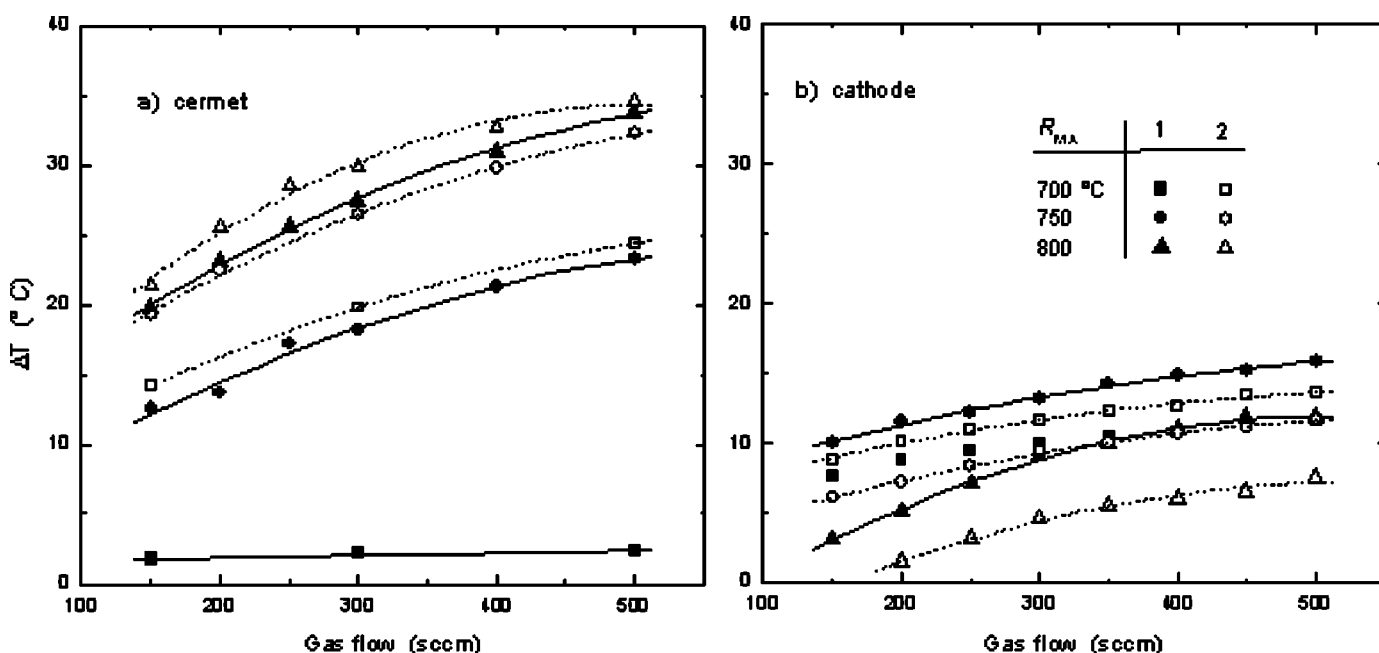


Figure 4. Overheating of YSZ platelets at various furnace temperatures either with (a) a single cermet or (b) a single cathode coating.

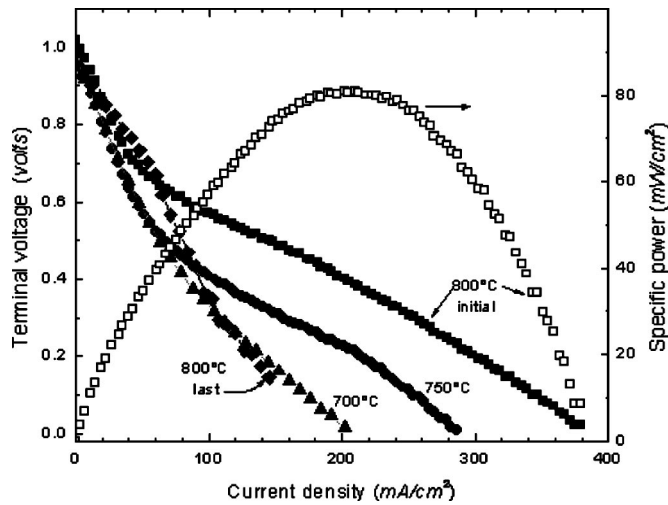


Figure 5. Typical polarization curves from an electrolyte-supported cell with a $\text{La}_{0.8}\text{Sr}_{0.2}\text{MnO}_3$ cathode and a 55Ni-45YSZ anode at 800°C, 350 sscm and $R_{\text{mix}} = 2$.

supported cells performed best immediately following initial cermet reduction. The maximum specific power and the short-circuit current are the most affected properties with time in contradistinction with the OCV which varies only slightly. Despite this aging phenomenon, additional useful observations could still be drawn from fresh cells made out of different cathode materials, in Fig. 6. LSMF22 behaves much like LSM20. The LSM50 cathode exhibits poor polarization properties, but this is attributed to a denser electrode because this material sinters much more easily than LSM20 during cell fabrication. Note also the lower values of R_{mix} in Fig. 6, $R_{\text{mix}} = 1$ representing a minimum for a satisfactory operation of these cells. Higher values of R_{mix} have been tested on a single cell in Fig. 7 up to $R_{\text{mix}} = 5$ with still a significant current drawn from that cell. The last curve at $R_{\text{mix}} = 2$ is again significant of the ageing process already mentioned above.

Anode-supported cells.—Figure 8 describes the effect of R_{mix} upon E_0 , the OCV of the anode-supported cells. E_0 reaches a maximum value in the vicinity of $R_{\text{mix}} = 2$. It then slowly decreases as

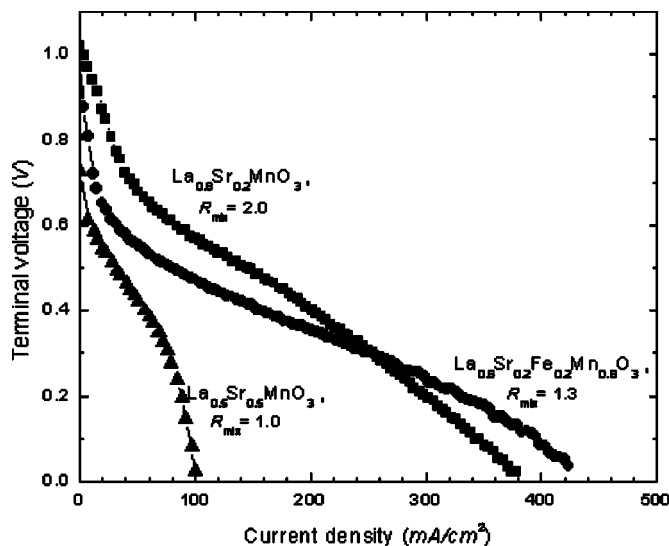


Figure 6. Initial polarization curves at 800°C from various electrolyte-supported cells with different cathode compositions and R_{mix} ratios.

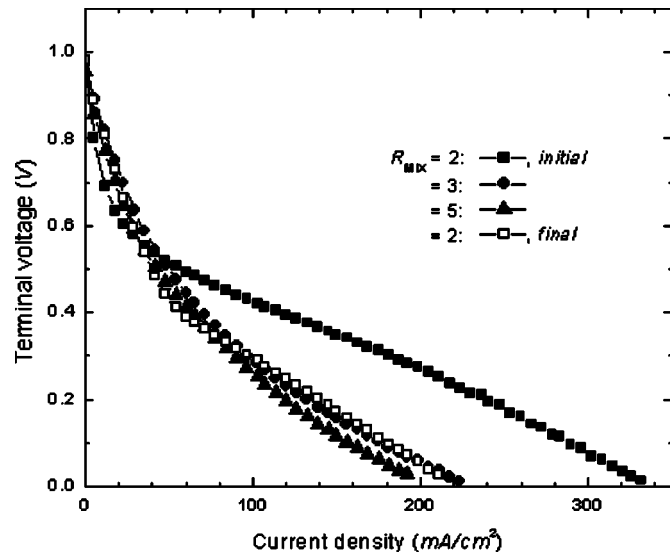


Figure 7. Successive polarization curves from an electrolyte-supported cell with a $\text{La}_{0.8}\text{Sr}_{0.2}\text{MnO}_3$ cathode and a 55Ni-45YSZ anode at 800°C and various R_{mix} ratios.

R_{mix} is lowered and drops abruptly as R_{mix} reaches 0.5. The data in parentheses indicate that these are not yet fully stabilized at this latter value which also corresponds to the theoretical full stoichiometric combustion of the methane-air mixture. At $R_{\text{mix}} = 0.5$ and below, the cell operation should become severely limited by an eventual cermet reoxidation. The normal operating range of the cells should stand between $0.5 < R_{\text{mix}} \leq 2$. Additional data are provided above $R_{\text{mix}} = 2$ mainly to document the actual cell behavior. Various polarization curves were drawn for an anode-supported cell in Fig. 9. There is drastic improvement in performances in comparison to the electrolyte-supported cell from Fig. 5. The maximum current to be drawn from the anode-supported cell is also highly dependent upon the magnitude of the gas flow. It increases very significantly from 410 mA/cm^2 at 150 sscm to above 1.0 A/cm^2 at 350 sscm and $R_{\text{mix}} = 0.88$.

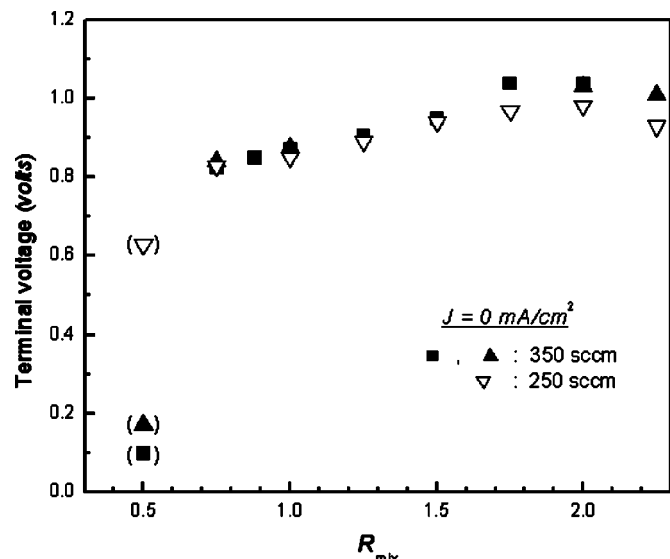


Figure 8. Open voltage values as a function of the methane-to-oxygen ratio for three different anode-supported cells at 800°C.

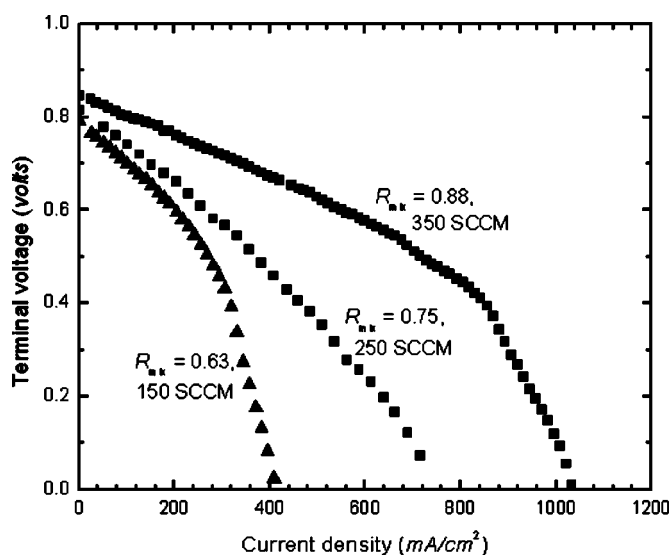


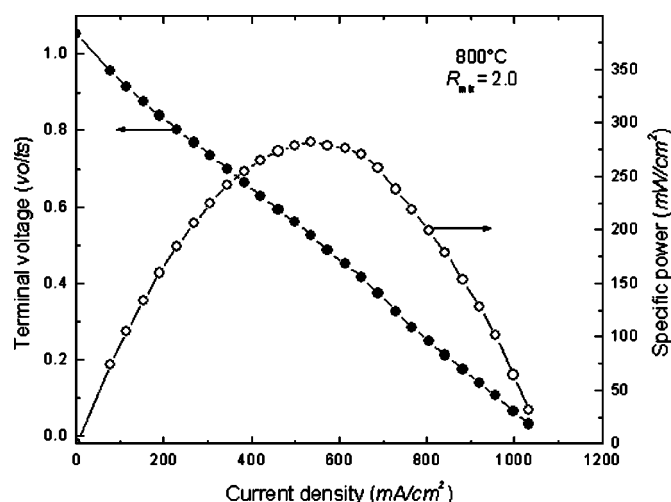
Figure 9. Polarization curves from an anode-supported cell for various gas flows and methane-to-oxygen ratios at 800°C.

At $R_{\text{mix}} = 2$, under 350 sccm (Fig. 10a), the specific power density is about 280 mW/cm² at 800°C. In Fig. 10b, a comparison of the cell performances is made for two different temperatures. The maximum specific power achieved at 800°C reaches 360 mW/cm² while the cell still performs satisfactorily at 700°C with a maximum specific power of about 290 mW/cm². The specific power at $R_{\text{mix}} = 2$ at 800°C is still quite close to the preceding value of 360 mW/cm² but higher than for electrolyte supported cells. Aging occurs at a much slower rate with this latter type of cell, thereby allowing full characterization of all cell operating parameters without any major difficulty. In Fig. 11, the OCV is shown not to evolve significantly with time. When a constant current load equal to 600 mA/cm², fairly close to the maximum specific power available, is applied, the voltage drops by about 20% after 15 h of test duration.

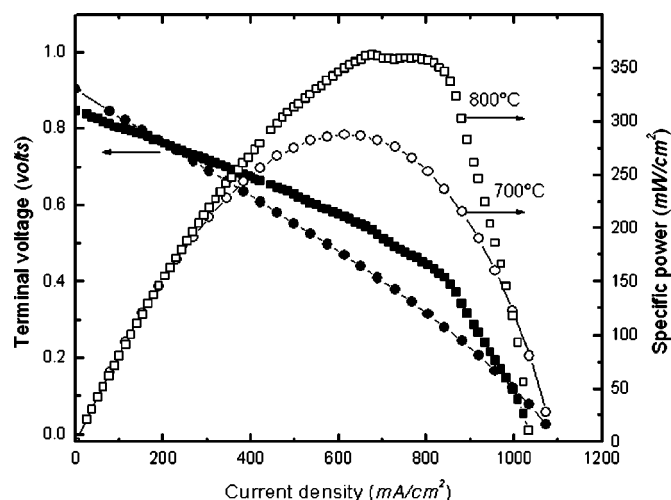
Discussion

Overtemperatures.—Based on the results from the blank samples, no significant methane combustion within the present experimental set-up takes place before the methane-air mixture reaches the cell chamber. Any temperature rise would come from the presence of catalytic components being parts of the actual cells. In the case of Hibino and coworkers, the additional use of platinum makes their so-called cell operating temperatures somewhat dubious. These temperatures should be considered, as here, as preset furnace temperatures with the additional effect of platinum. One of their most recent papers is accordingly on the temperature rise close to certain cells.¹⁸ Platinum has been shown elsewhere¹⁰ and here to have by far the largest effect upon expected cell temperatures. For this latter material, our own overtemperature measurements are in agreement with those from these authors.¹⁸ In addition, they do indicate that no large departures from preset temperatures are expected for our own cells at 800°C and even more evidentially at 700°C.

Operating range and safety limits.—No useful reactions are expected outside the range $0.5 \leq R_{\text{mix}} \leq 2$. This range corresponds to methane concentrations of 12.8 to 29 vol % in air. Studying this full range as done here is mainly useful to more completely document the actual cell behavior. Nonetheless, there is no doubt that caution should be exerted while handling such mixtures. The explosivity limits of methane-air mixtures have already been discussed by Hibino *et al.*²² in regard to single-chamber fuel cells. At room temperature, the unsafe region would stand between 5 and 15 vol % methane in air and this region widens as temperature is increased. In our own set-up, one should note, among other means, the lack of



(a)



(b)

Figure 10. (a) Polarization curve of an anode-supported cell with $R_{\text{mix}} = 2$ under 350 sccm and at 800°C. (b) Effect of temperature upon polarization and specific power of an anode-supported cell at 350 sccm. R_{mix} equals 1.0 and 0.88 at 700 and 800°C, respectively.

any dead volume, a constant mixture flow, the relatively small gas quantities involved, and the presence of a nitrogen purge. That permitted us to investigate the full R_{mix} range indicated above without any major difficulties. On the other hand, a full application of the single-chamber SOFC would have to take the above parameters into consideration and, most probably, new intrinsically safe designs.

Fuel cell performances.—The best cell performances within the present study were achieved with the anode-supported cells. A good indication of the cell morphology is to be found in the technical data of InDEC B.V. for their so-called ASC-LSM cell. The corresponding state-of-the-art fabrication does not imply exotic materials, but rather the use of graded layers for both electrodes, a very thin YSZ electrolyte layer and the incorporation of YSZ particles into the cathode close to the interface. A comparison is made in Table I between our results, no. 6 and 7, and those previously obtained by Hibino and coworkers with platinum collectors at the anodes, no. 1 to 5. Our electrolyte-supported cells compare favorably with the cells in no. 1, made out of approximately the same materials, if the difference in furnace temperature is taken into account. It has been mentioned before that the addition of 15 wt % MnO₂ in cells 2 and 3 could provide an additional catalytic effect⁷ although it is far more

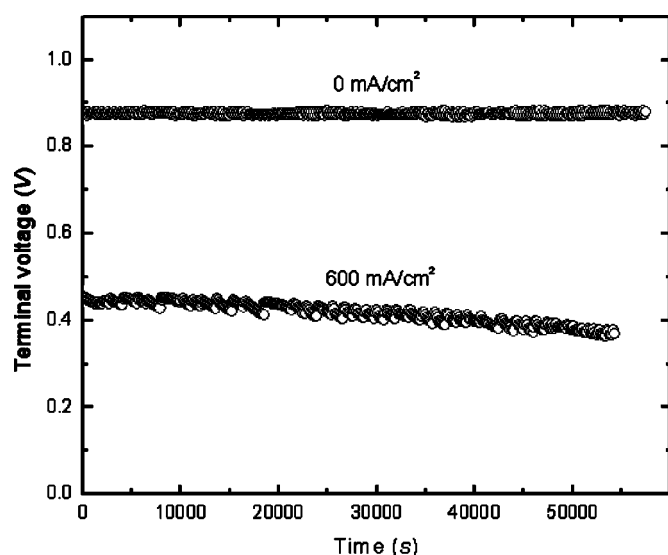


Figure 11. Aging of an anode-supported cell at 800°C at OCV and under a constant current load equal to 600 mA/cm². $R_{\text{mix}} = 2$ and gas flow equal to 350 sccm.

obvious that it creates a diphasic material and that it accordingly modifies the cathode morphology upon sintering. The anode-supported cells should be compared to no. 4 and 5 made out from more exotic electrode and electrolyte materials and having platinum collectors. The anode-supported cells compare quite favorably with cell no. 4. Cell no. 5 still delivers unsurpassed performances. PdO in cell no. 5 was mentioned to promote methane partial oxidation.⁸ It is also most probable that it adds to the methane oxidation promotion by platinum to strongly modify the actual operating temperature of this latter cell.

Within the working range of the cells, the OCV E_0 tends to increase with an increase in R_{mix} and also with a decrease in temperature. This stands for all the cells mentioned in Table I. For the electrolyte-supported cells, E_0 reaches a maximum of 1.0 V at $R_{\text{mix}} = 2$. According to Eq. 5, this would also correspond at 800°C to an oxygen partial pressure roughly equal to 10^{-20} atm at the anode/electrolyte interface, thus to poorly buffered conditions at that interface. As soon as a current is drawn, the so-formed products initially induce a more rapid change in $(p_{\text{O}_2})_a$ and, a consequently more rapid voltage drop. As far as specific power is concerned, it seems that the anode-supported cells work as well within the single-chamber as within the conventional two-chamber configuration. A maximum specific power of 270 mW/cm² at 700°C is reported for

the same cell fabrication in a two-chamber configuration²¹ in comparison with a value of 285 W/cm² obtained within this study. Until now, however, the fuel utilization for the single-chamber cell still remains quite low. Use is made of Eq. 6 and the various parameters accompanying Hibino's cell no. 5 in Table I; methane-air mixture at 300 sccm and $R_{\text{mix}} = 1$, electrode area equal to 0.63 cm². Although there is some uncertainty upon the actual cell operating temperature, that does not significantly affect ΔH_{react} and, thus, the resulting figure. One ends then with a fuel utilization factor equal to 3.6%. That figure can eventually be almost doubled by a more efficient use of the mixture flow on the cathode side.

In improving cell performances, other factors beside cell materials require closer attention. Current collection is one of these. Another important factor relates to the actual flow path of the incoming mixture around the cell including electrode surface areas and mixture recycling. As to aging of our electrolyte-supported cells, several factors could contribute to that effect. One is carbon deposition. However, these cells do not seem to degrade more rapidly at higher R_{mix} values while carbon has not been evidenced yet on any of them. Another factor would be post-sintering of the nickel contained within the cermet initially reduced at 800°C with a corresponding reduction of its specific surface. Such a process would be initially very active and would slow down progressively with time. Finally, it can also be speculated that electrode poisoning of the nickel electrode occurs through the surface diffusion of gold coming out from the current collector. This is to be understood quite differently from the cell degradation at 900°C already attributed to the melting of a gold-nickel eutectic.¹⁰ If nickel poisoning by gold was to be active, it would be expected to work much more slowly with much thicker anodes pertaining to the anode-supported cells. In fact, such thicker anodes offer far better resistance to aging. Distinct diffusivities between the various gaseous species towards the anode/electrolyte interface may also act differently in the case of thicker electrodes. All factors above are presently under study for further improvement of the single-chamber cells with special attention being given to chemical analysis of the exiting gases.

Conclusion

Special care has been taken within this study to the gas flow around single-chamber cells and to current collection. The electrolyte and anode-supported cells, made mostly of conventional materials, have been tested under methane-to-oxygen ratios ranging from about 0.6 to 5.0 and temperatures between 700 and 800°C. Within the present study, true cell operating temperatures should not depart widely from nominal furnace temperatures, in contradistinction to cells utilizing catalytically active noble metals. Large short-circuit currents could be drawn from these cells, especially in the case of the anode-supported cells. These cells also had by far the highest maximum specific power, reaching 360 mW/cm² at 800°C. Aging is

Table I. Various single-chamber cell performances in methane-air mixtures. (Percentages are given per weight and GDC20 stands for $\text{Ce}_{0.8}\text{Gd}_{0.2}\text{O}_2$; the other notations are as defined.)

No.	T° (°C)	R_{mix}	Electrolyte	Anode	Cathode	P_{max} (mW/cm)	$I_{V=0}$ (mA/cm)	E_0 (V)	Ref.
1	950	1	8YSZ	Ni-8YSZ	LSM20	121	550	0.80	7
2	950	1	8YSZ	Ni-25%GDC20	LSM20	162	780	0.83	7
3	950	1	8YSZ dipped into (MnNO_3) ₂	Ni-25%GDC20	+15% MnO ₂ LSM20	213	1170	0.85	19
4	700	1	LSGM	Ni-10% SDC20	SSC50	355	n.a.	0.92	20
5	550	1	SDC20	Ni-30%SDC20 +1%PdO	SSC50	644	n.a.	0.90	8
6	800	2	8YSZ	55% NiO- 8YSZ	LSM20	85	380	1.0	10, This study
7	800	.88	8YSZ	NiO-YSZ	(La, Sr)MnO ₃	360	1200	0.86	This study

mostly acute for the electrolyte-supported cells. Ways of interpreting the various undergoing phenomena in unstable methane-air mixtures have been suggested. Ways of improving the present cell efficiency are also currently envisaged.

Acknowledgments

The authors thank the Natural Sciences and Engineering Research Council of Canada and the Hydro-Québec Research Institute for financial support. The technical assistances from Jean-Paul Lévesque is greatly appreciated.

References

1. C. Eyraud, J. Lenoir, and M. Géry, *C.R. Acad. Sci. Paris*, **252**, 1599 (1961).
2. W. van Gool, *Philips Res. Rep.*, **20**, 81 (1965).
3. T. Hibino and H. Iwahara, *Chem. Lett.*, **7**, 1131 (1993).
4. T. Hibino, K. Ushiki, T. Sato, and Y. Kuwahara, *Solid State Ionics*, **81**, 1 (1995).
5. G. A. Louis, J. M. Lee, D. L. Maricle, and J. C. Trocciola, U.S. Pat. 4,248,941 (1981).
6. K. Asano and H. Iwahara, *J. Electrochem. Soc.*, **144**, 3125 (1997).
7. T. Hibino, S. Wang, S. Kakimoto, and M. Sano, *Electrochem. Solid-State Lett.*, **2**, 317 (1999).
8. T. Hibino, A. Hashimoto, M. Yano, M. Suzuki, S. Yoshida, and M. Sano, *J. Electrochem. Soc.*, **149**, A133 (2002).
9. L. Bay, T. Horita, N. Sakai, M. Ishikawa, K. Yamaji, and H. Yokokawa, *Solid State Ionics*, **113–115**, 363 (1998).
10. T. W. Napporn, F. Morin, and M. Meunier, *Electrochem. Solid-State Lett.*, **7**, A60 (2004).
11. I. Riess, P. J. van der Put, and J. Schoonman, *Solid State Ionics*, **82**, 1 (1995).
12. Y. Shiratori and Y. Yamazaki, *Electrochemistry (Tokyo, Jpn.)*, **69**, 92 (2001).
13. S. Raz, M. J. G. Jak I. Riess, J. Schoonman, and I. Riess, *Solid State Ionics*, **149**, 335 (2002).
14. A. J. Appleby, *J. Power Sources*, **49**, 15 (1994).
15. K. Asano, T. Hibino, and H. Iwahara, *J. Electrochem. Soc.*, **142**, 3241 (1995).
16. Outokoumpu HSC Chemistry, Version 4.1, Pori, Finland (2000).
17. S. Primdahl, Ph.D. Thesis, University of Twente, Twente, The Netherlands (1999).
18. T. Hibino, A. Hashimoto, T. Inoue, J. Tokuno, S. Yoshida, and M. Sano, *J. Electrochem. Soc.*, **148**, A544 (2001).
19. T. Hibino, H. Tsunekawa, S. Tanimoto, and M. Sano, *J. Electrochem. Soc.*, **147**, 1338 (2000).
20. T. Hibino, A. Hashimoto, T. Inoue, J. Tokuno, S. Yoshida, and M. Sano, *J. Electrochem. Soc.*, **147**, 2888 (2000).
21. P. Nammensma, J. P. Ouweltjes, G. van Druiten, B. Rietveld, and R. Huiberts, Paper presented at Fuel Cell Seminar 2002, Palm Springs CA, Nov 18-21, 2002.
22. T. Hibino, S. Wang, S. Kakimoto, and M. Sano, *Solid State Ionics*, **127**, 89 (2000).